Dissociative Grazing Scattering of H2+ Ions from Metal Surfaces†

ARTICLE *in* THE JOURNAL OF PHYSICAL CHEMISTRY B · JULY 2002

Impact Factor: 3.3 · DOI: 10.1021/jp020671e

Dissociative Grazing Scattering of H_2^+ Ions from Metal Surfaces†

Igor Wojciechowski,‡ Marina Medvedeva,‡ Barbara J. Garrison,‡ Vladimir K. Ferleger,§ and Werner Heiland*,||

Department of Chemistry, The Pennsylvania State University, University Park, Pennsylvania, 16802, Arifov Institute of Electronics, Tashkent 700143, Uzbekistan and Fachbereich Physik, Universität Osnabrück, Barbarastr. 7, D-49069 Osnabrück, Germany

Received: March 11, 2002; In Final Form: May 30, 2002

Energy distributions of H atoms resulting from grazing scattering of H_2^+ from metal surfaces are calculated analytically and by using classical trajectories simulations. The main mechanism leading to dissociation of H_2^+ is proposed to be dissociative capture of an electron from the metal into the antibonding state of the H_2 molecule. It is shown that the energy distributions of scattered atoms yield information of both the molecular axis orientation and the vibrational excitation of the molecules during the scattering process.

1. Introduction

The interaction of fast keV molecules with solid matter has been investigated over past two decades in order to obtain both a fundamental view of the molecule−surface interaction and to develop an analyzing tool in a variety of fields such as heterogeneous catalysis, environmental chemistry, modification of materials, and erosion of space vehicles.[1] At small glancing angles, a so-called perpendicular energy, $E_\perp$, of the primary beam, where $E_\perp = E_0 \sin^2 \alpha_0$, with E_0 the initial energy and α_0 the glancing angle, of below 10 eV can be achieved. Such energies are typical for the activation of chemical reactions on a surface. Thus, the use of grazing scattering of molecules with an initial energy E_0 of the order of several keV enables us to obtain the physics of particle−surface interactions in the low energy region. This approach is especially applicable for simple molecules such as hydrogen because it is difficult to obtain beams of light molecules at hyperthermal energies.[2] Neutral swift molecules have been obtained in at least three groups[3−5] using neutralization in a gas cell.

From the experiments, it has been established that, for the energy range of initial energies of $E_0 \approx 0.1-10$ keV and glancing angles of $\alpha_0 \leq 10°$ with respect to the surface, both intact molecules and H atoms resulting from molecular dissociation can be detected in the scattered flux.[1] The main question is which mechanisms cause the molecules H_2 and H_2^+ to dissociate.

Various mechanisms including collisional processes,[6−8] electron transitions,[9−11] and action of adsorption forces[12] have been proposed to cause dissociation. At present, it is clear that the relative contribution of the different dissociation processes depends on the charge state of the bombarding molecules, the geometry of scattering, and the properties and structure of the target surface. The majority of studies have concluded that the main mechanism causing H_2^+ ions to dissociate is the electron capture from a metal into the antibonding state of the molecule[13−15] followed by dissociative neutralization. For the bombardment by neutral H_2 molecules, this channel is closed. Nevertheless, dissociation of H_2 in the case when the perpendicular energy is less than the dissociation energy of the molecule[16] can be connected with the adsorption forces. Another factor responsible for H_2 dissociation is a weakening of the H_2 bond near the metal surface due to screening by the electron gas.[16,17] This idea is supported by the experiments in ref 16. Rechtien et al.[18] proposed that, although a majority of H_2^+ ions are neutralized into the repulsive state, a significant fraction of those molecules have sufficient time to undergo Auger deexcitation into the ground state before the atoms can separate along the repulsive potential energy curve. Therefore, the mechanisms of H_2 dissociation can also have an effect on the molecular yield in the case of H_2^+ ions.

Varying the work function of the sample by adsorbing alkali metal atoms can change the charge exchange between the H_2^+ ion and the surface. Additional neutralization channels into excited states of H_2 can become open. For example, electron capture into the $c^3\Pi_u$ state of H_2 followed by Auger decay into the ground state can decrease the number of dissociation events.[16]

Significant information on dissociation mechanisms and the state of the molecule at the moment of dissociation are contained in the energy distributions of the scattered atoms. Experiments[19−21] have shown that the energy spectra of atoms scattered from a solid surface due to molecular ion bombardment are broadened in comparison with those from atomic ion bombardment and have extended high energy tails beyond the incident energy per atom. A typical experimental spectrum of scattered neutral species converted from a time-of-flight measurement is shown in Figure 1. The experimental detector records all of the neutral particles as a function of time. To create an energy spectrum, an assumption must be made about the mass of the particles. In the case of Figure 1, it has been assumed that all of the particles have the mass of the incident H_2 molecules. The total spectrum is a superposition of at least two distributions. The conventional interpretation of the spectrum is that the surviving molecules form the "hat" of the distribution near $E/E_0 \approx 1$. At higher and lower energies, dissociated atoms contribute to the spectrum. The remaining broad part of the spectrum has a

† Part of the special issue "John C. Tully Festschrift".

* To whom correspondence should be addressed. E-mail: wheiland@uos.de.

‡ Department of Chemistry, The Pennsylvania State University.

§ Arifov Institute of Electronics.

|| Fachbereich Physik, Universität Osnabrück.

10.1021/jp020671e CCC: $22.00
Published on Web 07/03/2002

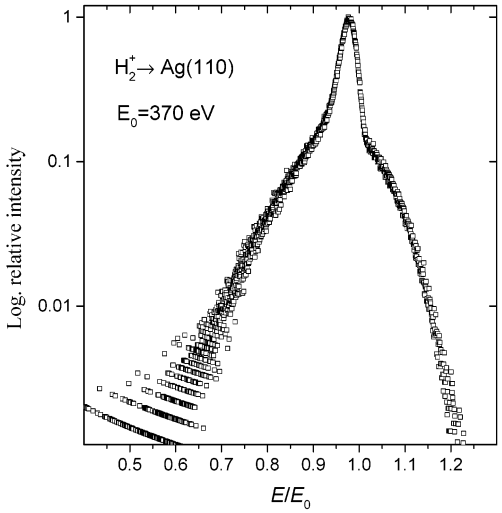

Figure 1. Total energy spectra of neutral H_2 and H scattered from Ag(110). The glancing angle of H_2^+ projectiles is 3°, and the total scattering angle is 6°. Surviving H_2 molecules form the central contribution in the spectra or the "hat". Hydrogen atoms produced by dissociation form the broad underlying distribution.

pronounced asymmetry. The low-energy tail is well described in terms of energy loss and energy loss straggling for the atoms penetrating deeper into the bulk and traveling longer inside the solid.[22] The focus of our study is the high-energy tail.

It is clear that the high-energy tails result from either redistribution of the energy of the atoms colliding with each other after dissociation or the kinetic energy release in the molecular center of mass system that is linked to the energy in the laboratory frame by a Galilean transformation. The first possibility is considered in refs 23 and 24, where it has been shown that this channel is only effective for heavy particles and large glancing angles. For grazing scattering, the broadening of the energy spectra is connected with the energy release, ϵ, which depends on the electronic structure of the molecule as well as its excitation and molecular axis orientation at the moment of decay. Indeed, the energy E_1 of an H atom from a molecular ion dissociating at some point of its scattering trajectory can be obtained by a Galilean transformation as

$$E_1 = E_i + \frac{\epsilon}{2} \pm \sqrt{2E_i\epsilon}\cos\theta\sin\varphi \qquad (1)$$

where E_i is the kinetic energy of the atoms at the moment of dissociation, which is less than E_0 due to energy losses, θ and φ are the polar and azimuthal angles determining the molecular axis orientation in the frame with the polar axis directed along the velocity vector, and ϵ is the energy released in the center-of-mass system of the molecule.

In general, there is a spectrum of energies ϵ described by a corresponding distribution function $f(\epsilon)$. The determination of the form of this function, which is closely connected with the dissociation mechanism, is important for the latter to be identified. In the case when the form of the function $f(\epsilon)$ is deconvoluted from the energy distributions of the scattered atoms, the most convenient part of the spectra for solving this task is the high energy tail. The particles that give rise to higher tails arise from particles whose trajectories lie above the surface and are thus less blurred by multiple scattering, inelastic losses, and energy loss straggling.

Another factor affecting the form of atomic energy distributions is the position of the molecular axis with respect to the translational velocity vector at the moment of dissociation. The initial uniform random distribution of axis orientation in space is changed when the molecules are interacting with the surface. As it is seen from eq 1, for molecules oriented parallel to the translational velocity, the energy spectrum should have a double-peak structure corresponding to the forward and backward movement of fragments with respect to the center-of-mass of the dissociating molecule. Such a structure, indeed, was observed in the experiments of 400 keV H_2^+ scattering from W surfaces[25] because of the alignment of the axis parallel to the surface, but it has never been seen for slow molecules. A one-peak distribution can be produced if molecules are oriented perpendicular to the velocity vector. Such orientation can be a result of a so-called propeller mode excitation, which has been observed in calculations for molecules scattered along surface semichannels.[8,26] The term propeller mode was suggested in refs 8 and 26 for rotational movement in which the angular momentum vector is aligned with the beam direction. The most effective approach to treat the molecular scattering problem is molecular dynamics or classical trajectory calculations. Classical trajectory simulations of H_2 and N_2 scattering from metal surfaces have been carried out previously.[21,26,27] No electronic dissociation processes were considered in these studies. If only mechanical dissociation of the molecule was taken into account, the fraction of dissociated molecules was underestimated, even in the case of chemically inert N_2 molecules. A successful attempt to improve the results of the classical simulations was undertaken in ref 21, where a weakening of the intramolecular bond was introduced as a function of the electron density of the surface as sampled by the N_2.

The aim of the present work is to derive the information contained in the energy distributions of hydrogen atoms formed in the process of the dissociative scattering of H_2^+ molecular ions from a metal surface, including the dependence on the dissociation mechanism, the axis orientation, and the state of vibrational excitation of the molecules at the moment of their decay. To tackle this problem, we use both analytical estimations of the high energy tails and a classical trajectory study of the scattering systems H_2^+−Ag(110) and H_2^+−Pt(110).

2. Models

We present two models for the calculation of kinetic energy distributions of scattered H atoms. Unambiguous connection between the energy released in the dissociation event and the shape of high energy tails allows us to develop a simple calculation model described in section 2.1. Molecular dynamics calculations described in section 2.2 display more features in the molecule-surface scattering events.

2.1. Analytical Calculations of High-Energy Tails. A model for the calculation of the high-energy tail of the energy distributions proposed here is based on the following assumptions.

(1) The dissociative neutralization process for H_2^+ for the energies and angles under study is supposed to be the only one causing the molecules to dissociate. Both experimental data[28,29] and calculations[30,31,32] indicated a dominating role of this process. In this mechanism, the kinetic energy ϵ released in dissociation is determined by the separation distance R between the atoms in the molecule at the moment of the electron transition occurring at a fixed nuclei position. The function $f(\epsilon)$ is

$$f(\epsilon) = \left.\frac{dN}{dR}\right|_{R=R(\epsilon)} \frac{dR(\epsilon)}{d\epsilon} \qquad (2)$$

where $R(\epsilon)$ is determined by the form of the repulsive potential curve for the $b^3\Sigma_g^+$ state of H_2. This state is well approximated by an exponential function

$$U(R) = A \exp(-\alpha R) \tag{3}$$

The distribution function, dN/dR, is calculated within the harmonic oscillator approximation for the ground state of H_2^+. Besides a constant factor, the function $f(\epsilon)$ is[33]

$$f(\epsilon) = \frac{1}{\epsilon} \exp\left[-\frac{m\omega}{\hbar\alpha^2}\left(\ln\frac{\epsilon}{A} + R_0\alpha\right)^2 \tanh\left(\frac{\omega\hbar}{2kT_v}\right)\right] \tag{4}$$

where m, ω, R_0, h, and k are the atom mass, the vibrational frequency, the equilibrium separation, and the constants of Planck and Boltzmann, A and α are the parameters of the potential energy curve, and T_v is the vibrational temperature.

(2) As the high energy tail of a spectrum where $E/E_0 > 1$ cannot be formed by molecules and atoms penetrating the solid where inelastic energy losses and energy loss straggling are relatively high, the effect of straggling on the form of the high energy part of the spectra may be neglected. Inelastic energy losses determined by the dependency $\Delta E \propto E_0$[34−36] can be simply considered by the corresponding shift of the spectra toward lower energies.

(3) Both experimental data[28,29] and results of the calculations[30−32] are consistent with the conclusion that the rate of the dissociative neutralization is greater than 10^{14} s^{-1}. Consequently, the decay of the molecules occurs on the initial part of the scattering trajectory before the turning point.

On the basis of the above considerations, we choose $E_i = E_0$ and describe the whole molecule prehistory, before its decay, with T_v, as a model parameter. Therefore, the high-energy tails can be estimated by the formula

$$\frac{dN}{dE} \sim \int \delta[E - E_1(\epsilon,\Omega)] f(\epsilon)\, d\Omega \tag{5}$$

where $\delta(x)$ is the Dirac delta function. The integration is made over the solid angle Ω of the detector. As the electron transition into the antibonding state mainly occurs on the initial part of the trajectory, all molecular axis orientations are assumed to be equally distributed.

2.2. Molecular Dynamics Simulations. The scattering of H_2^+ from a Ag(110) surface at a glancing angle of 3° along two directions, [1$\bar{1}$0] and at an azimuthal angle $\phi = 10°$ off the [1$\bar{1}$0] direction (a pseudo random direction) is modeled using molecular dynamics computer simulations described in great detail earlier.[37,38] The primary energy of molecules is varied from 200 to 1600 eV. The surface is composed of a periodically repeated lattice of 25 × 18 atoms arranged in seven layers. No defects or adsorbates are taken into account.

To set a temperature of the crystal, the interaction among all metal atoms is described by a MD/MC−CEM many body potential originally designed by Kelchner et al.[39] Before the simulations were started, the sample was relaxed to 300 K for 10 ps to allow it to approach a thermal equilibrium. The generalized Langevin equation method[40] was applied to the bottom four layers in order to maintain the upper three atomic layers at constant temperature. The initial bonded state of the H_2^+ molecule is described by a Morse potential with the parameters set as follows: the binding energy D is 2.78 eV, the equilibrium distance r_e is 1.06 Å, and the exponential factor β is 1.33 $Å^{-1}$.[41] The potential cutoff distance r_{max} is 3.5 Å. The triplet repulsive state of the H−H system is modeled by the exponential function eq 3 with the parameters A having a value of 43.38 eV and α equal to 2.6 $Å^{-1}$, values which represent a best fit of the experimental data.[41] The H−Ag interaction is described by a pair repulsive Moliere potential with a Firsov screening length.[42] The image force potential $u = e/4(x_{cm} - x_i)$, where e is the elementary charge, x_{cm} and x_i are the distances between the surface and the molecule center-of-mass and the image plane, respectively, acts between H_2^+ and the surface. The electronic boundary of the solid should be at a distance of half a lattice constant above the plane containing centers of mass of surface atoms. In this respect, a value of $x_i = 1$ Å is chosen for the calculations.

Hamilton's equations were solved for 5400 H_2^+ scattering events. The initial molecule axis orientation is randomly chosen from a uniform distribution in space. Both energy and angle spread for the H_2^+ projectiles seem to have a small effect on energy spectra of hydrogen atoms and were not taken into consideration. To simulate the experimental situation where H_2^+ molecules are formed in an ion source by electron impact ionization of H_2, an amount of internal energy of 0.7 eV was added to each molecule.[26] Electronic energy losses and their straggling were neglected. The former effect can be considered by shifting the spectra to lower energies. Straggling, as discussed earlier, only has an effect on the low energy tails of the spectra.

We assume that the initially charged hydrogen molecule can undergo an electron capture on its scattering path. The electron can be captured either into the ground-state $X^1\Sigma_g^+$, or the lowest excited triplet state $b^3\Sigma_u^+$.[30−32] Because we are interested in the energy spectra of scattered H atoms, we neglect the former possibility and introduce the rate of the electron capture into the triplet state as

$$W = B \exp[-\gamma(x_{cm} - x_i)] \cos^2\chi \tag{6}$$

where χ is the angle between the molecular axis and the perpendicular to the surface. This dependence was found in first principles calculation[30−32] to be a good approximation for H_2^+ neutralization on Al for not too small molecule−metal separation distances. We used the same parameters for the H_2^+−Ag system as obtained for H_2^+−Al in ref 31.

On each integration step, a decision of whether neutralization occurred or not is made according to the probability $P = \exp(-W\Delta t)$, where Δt is the integration step. Once the neutralization takes place, the H−H^+ interatomic potential is switched to the pure repulsive H−H potential eq 3. The image forces are switched off at this moment. The integration of any trajectory is either terminated when scattered species are 5 Å above the surface or switched on when a cutoff time of 200 fs was reached. In these latter cases, the hydrogen atoms remain inside the crystal.

3. Results and Discussion

In section 3.1, we discuss the results of molecular dynamics calculations, which predict the nature of the scattering changes as a function of incident energy for two azimuthal directions of the primary beam. In section 3.2, the vibrational states of the H_2^+ molecules at the moment of their dissociation on Pt(110) and Ag(110) surfaces are analyzed using the analytical method proposed above.

3.1. Molecular Dynamics Simulations. Calculated kinetic energy distributions of H atoms resulting from H_2^+ scattering at three initial energies 2$\bar{0}$8, 1059, and 1570 eV on Ag(110) along the low indexed [1$\bar{1}$0] direction ($\phi = 0°$) and random ($\phi = 10°$) direction are shown in Figures 2 and 3 along with the experimental data obtained under the same conditions. The calculated distributions are largely symmetric but have different

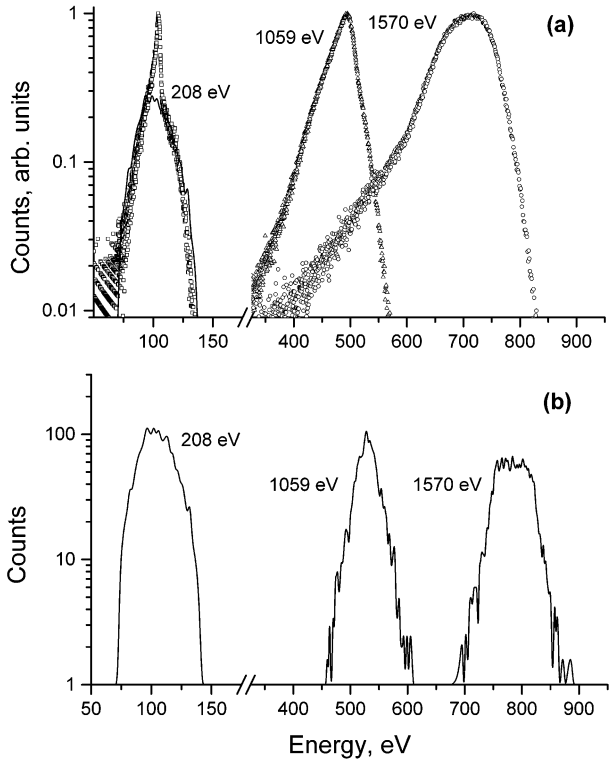

Figure 2. Kinetic energy distributions of H + H_2 for the scattering of H_2^+ incident on Ag(110) at a glancing angle of 3° along the [110] azimuthal direction obtained (a) in TOF experiments and (b) in molecular dynamics calculations. The initial energies of H_2^+ projectiles are shown in the plot. The calculated spectrum for 208 eV, transformed as discussed in the text, is also shown in the upper frame for comparison.

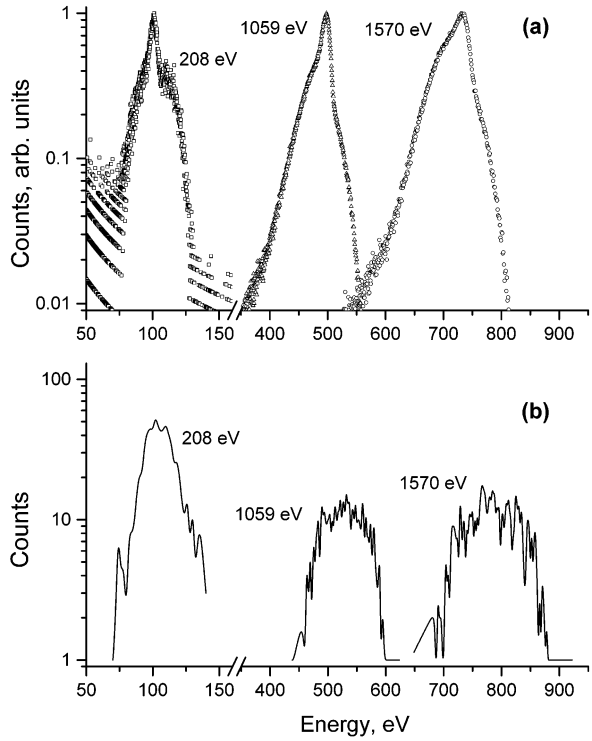

Figure 3. Same as for Figure 2, but for the random azimuthal direction (10° with respect to [1$\bar{1}$0]).

shapes for the cases in question. The number of scattered atoms from dissociation events is significantly greater for the channeling direction, because the projectile molecules approach

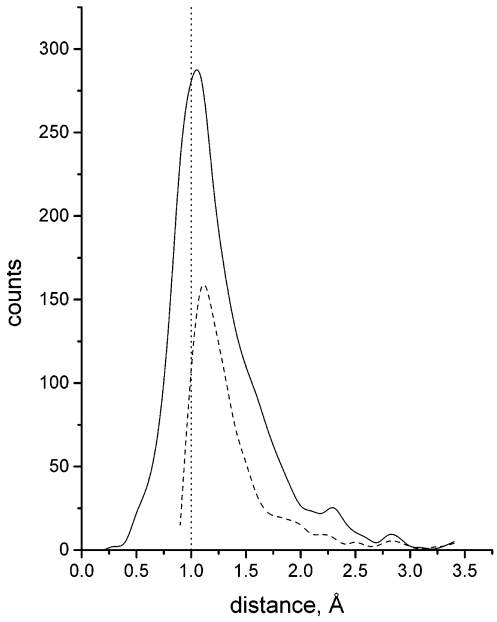

Figure 4. Distribution of dissociation events over the distances from the image plane for 1059 eV H_2^+. The solid line is for scattering along the [1$\bar{1}$0] direction. The dashed line is for the molecule.

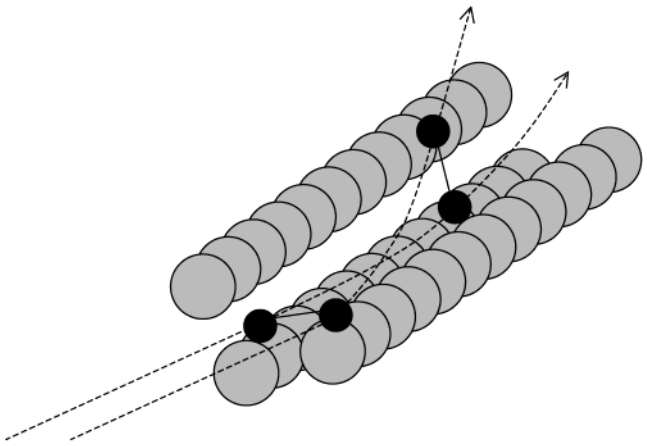

Figure 5. Scheme of molecular scattering along the surface semi-channel. Grey spheres are the target atoms. Black spheres represent the initial and upright positions of the hydrogen molecule.

closer to the surface along the channeling direction compared to the random direction. According to eq 6, the molecules that approach closer to the surface have a greater chance to be neutralized. The distributions of dissociation events with distance to the image plane are shown in Figure 4 for the two directions. In the case of $\phi = 10°$, all of the dissociated molecules captured an electron at the distances $x_{cm} - x_i > 1$ Å. At the same time, many molecules moving along the [1$\bar{1}$0] direction are neutralized closer to the surface, $x_{cm} - x_i < 1$ Å.

For the energy of 208 eV, the distributions are very similar for the both azimuths. This observation is not unexpected because in both cases dissociative electron capture occurs outside the surface influence in the region of 1.5−3 Å above the image plane. As a result, the initial state of the H_2^+ molecules is not changed by the interaction with the surface at the moment of dissociation. The surface acts as a mirror, just reflecting H atoms, and not changing their distribution. A width and shape of the distribution are determined by both the energy released in dissociation (eq 1) and orientational dependence of the neutralization rate (eq 6). As the energy increases, the spectra for the two bombardment directions become different. For $\phi =$

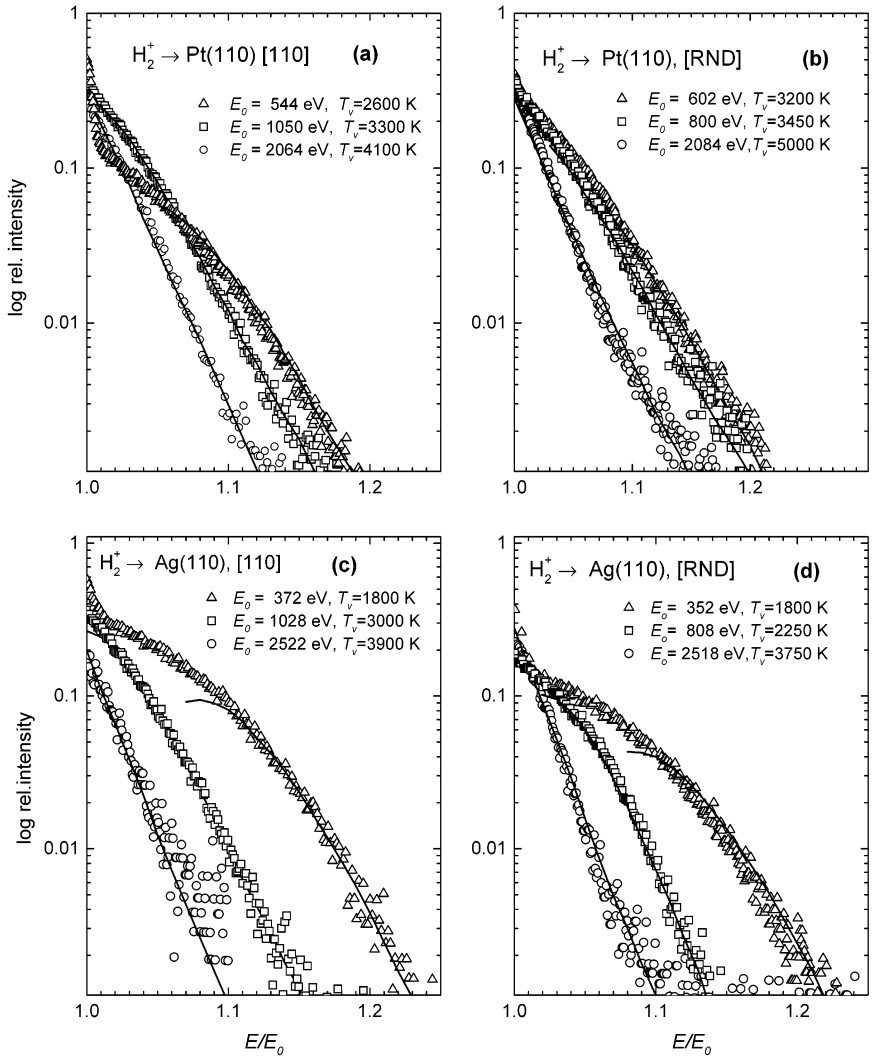

Figure 6. High energy tails of hydrogen atoms scattered from Pt(110) and Ag(110) under bombardment by H_2^+ molecules. Symbols are experimental values, and lines are the results from the calculations.

0°, the widths of the spectra are apparently less than those for the random direction. In the case of the channeling direction, H atoms with energies close to $E_0/2$ mainly contribute to the spectra. According to eq 1, it is a consequence of the fact that the axis of molecules producing these atoms was oriented normal to the velocity vector at the moment of dissociation. A reason for the relatively sharp peak in the distribution of atoms is connected with the specific rotational excitation, known as a propeller mode. This excitation was found in ref 8 to be effective for molecules moving along a surface semichannel. One of the atoms scattering on the channel ridge gains momentum perpendicular to the velocity vector direction. As a result, the torque vector is aligned with the translational movement direction, bringing the molecule to the upright position, Figure 5.

Although a straightforward quantitative comparison between the calculations and the experiment cannot be provided because of an unknown amount of survived molecules, a number of important conclusions can be derived from the calculations. A qualitative comparison can be made for the low energy scattering, where the extraction of the atomic spectra from the total experimental one can be easily done. That is shown in the upper frame of Figure 2, where the spectrum calculated for $E_0 = 208$ eV was normalized and shifted to lower energies by $\Delta E \approx 0.01E_0$. This value of inelastic energy losses is typical for surface scattering. The calculations reproduce the experimental atomic spectrum fairly well. Low energy molecules scatter on a rather smooth potential far enough from the surface. As a result, the energy loss straggling is minimal, and the energy spectra are practically symmetrical. With increasing primary energy, the asymmetry in the experimental spectra becomes visible because of straggling effects omitted in the calculations. At the same time, the shapes of the high energy parts of the calculated distributions are consistent with the experimental ones. Comparing the calculated spectra with the experimental data for the low-indexed channeling direction at 1059 eV, atomic scattering comprises most of the "hat". As a result, the central experimental peak becomes broader. It is especially pronounced when comparing the total experimental spectra for the two azimuthal directions. For 1570 eV, the central peak dominates in the spectrum for the channeling direction. As a consequence, the "hat" in the experimental spectrum is not distinguishable any more, because now it is a superposition of the narrow molecular peak with the broad atomic one centered at the same energy point. From our point of view, this disappearance of the "hat" cannot only be connected with increasing the inelastic energy losses and straggling for particles moving in the surface channels. Indeed, these effects should concern the low energy part of the spectra, and a long low-energy tail does appear in the spectrum for 1570 eV. Nevertheless, the high-energy part also changes, becoming smoother.

A contribution of the atomic distribution to the "hat" was found earlier in simulations[21] for N_2 molecules scattering on the Ag(110) surface along the low indexed direction. The model used by the authors of ref 21 for N_2 scattering included a weakening of the intramolecular binding forces by conduction band electrons near the metal surface. The scattering along the semichannels allows a penetration of N_2 molecules down to the second layer. Stronger screening in this case is expected, leading to the potential well between two N atoms to become extremely shallow. Consequently, dissociation with nearly zero kinetic energy release takes place. These "softly dissociated" fragments form the central narrow peak in the experimental energetic distribution. Because no screening is taken into account in the present calculation, the reason of the central peak appearance for the H_2^+-Ag scattering is connected with specific rotational excitation as mentioned above.

3.2. High Energy Tails. Equation 5 was used for the calculation of the high energy tails of the energy distributions under the conditions of the experiment,[43] i.e., for hydrogen atoms scattered from the surfaces of Pt(110) and Ag(110) at grazing incidence ($\alpha_0 = 3°$) of H_2^+ with the energy E_0 varying within the range 300 eV $< E_0 <$ 1300 eV. For a particular calculation, the function of the detector sensitivity was taken into consideration, and the integration over the angular variables in eq 5 was performed within the angle of acceptance of the detector of 1.2°.[43]

The high energy tails of scattered H atoms from Pt(110) and Ag(110) surfaces are shown in Figure 6 for three different incident energies and two incident angles. Also shown are the calculated spectra using eq 4 with inelastic energy losses assumed to be $\Delta E \propto E_0$. The adjustable parameter T_v was chosen to obtain a best fit with the experimental data. It is seen that the agreement between the theory and the experiment can be achieved by varying the only free parameter. One can interpret these fits as the vibrational temperature, T_v, of a molecule at the moment of its decay, determining the amount of energy released.

In the general case, a particular value of T_v at the moment of the molecule decay depends on many factors. First, after leaving the ion source, the beam of the bombarding molecules has a certain temperature resulting from both the type of the beam source and the physics of ionization.[26] In addition, as a result of multiple collisions of the molecule with the solid surface, the molecule can gain internal energy.[6]

It is clear that an amount of the internal energy accumulated by that way at the moment of the decay depends on the actual form of the scattering trajectory, i.e., E_0, α_0, the direction of the bombardment, the atomic structure of the target surface, and the electronic structure of the subsurface region determining the probability of the dissociation, i.e., roughly speaking, on the position of the decay point on the trajectory. It is not ruled out that the vibrational temperature can be changed by some electronic processes not connected with dissociation, for example, by the dependency of the equilibrium distance between the nuclei on the electron density near the surface.[8]

It is interesting to analyze the dependency of T_v on such experimental parameters as the initial energy and the type of the target surface and to consider the orientational sensitivity of T_v. The dependencies of T_v on E_0, giving the best fit between the calculated and experimental high-energy tails of H atoms scattered from Pt(110) and Ag(110) surfaces under bombardment with H_2^+ along the directions of [1$\bar{1}$0] and the random one, are shown in Figure 7. It is seen that T_v(Pt) > T_v(Ag) for all values of E_0, which can be explained by the fact that the Pt(110) surface is more corrugated and is known to reconstruct in the (1 × 2)-missing-row structure at room temperature. The actual structure in the experiments is (1 × 2) as shown by in situ LEED.[43]

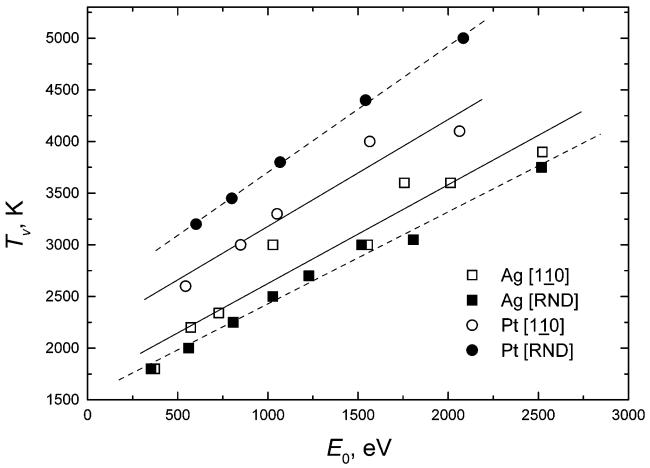

Figure 7. Dependences of vibrational temperature on the initial molecular energy fitted by linear functions. Open symbols are for the [1$\bar{1}$0] scattering, with circles on Pt(110) and diamonds on Ag(110). Solid symbols are for the random scattering, with squares on Pt(110) and triangles on Ag(110).

It is also seen from Figure 7 that the maximal value of T_v is about 5000 K; that is, the vibrational energy is ∼15% of the dissociation energy of the molecule. Therefore, the molecule cannot decay via vibrational excitation at least on the initial part of the scattering trajectory.

Another feature seen from Figure 7 is that the temperatures for scattering from Pt along the random direction are higher than for the [1$\bar{1}$0] direction. A possible reason is that the molecule moving along the trajectory experinces a more corrugated surface than for the low indexed direction, where it is mainly excited rotationally.[8] The difference in the temperatures is not so substantial for the scattering from Ag, especially for low initial energies. It seems to be connected with an approximately comparable corrugation for both directions. At the same time, the present MD simulations demonstrate (not documented here) that more energy goes into the internal degrees of freedom of H_2 molecules scattering along the [1$\bar{1}$0] direction than for the molecules moving along the high-indexed direction. The same feature was found in earlier calculation for the $H_2-Pd(110)$ system.[8] Thus, the process of vibrational excitation of the molecule results from the collisions of the molecule atoms with the target ones. The excitation energy gained might not be enough for the molecules to decay, but its amount affects the energy distribution of fragments resulting from electronic dissociation. Supposing the collisions to occur independently for the atoms having the energy E_i, the energy of each atom after the next collision will be proportional to E_i. Therefore, their relative energy determining the vibrational excitation of the molecule must also be proportional to E_i. The dependency $T_v \propto E_i$ is actually seen for the random directions for both Pt and Ag targets. The nonlinear behavior of the temperature with increasing E_0 for the channel direction may be connected with the additional contribution of rotational excitation to the dissociation of H_2^+ molecules.[26] In that case, the function $f(\epsilon)$ may differ from eq 4.

4. Conclusion

The calculations show that the observed form of the high energy tails of the spectra of H atoms scattered from Pt and Ag

under H_2^+ molecule bombardment can be described quite naturally, supposing the dissociative neutralization process to be a mechanism leading the molecule to dissociation. The values of the vibrational temperatures of the molecules at the moment of dissociation, obtained by fitting the calculated high energy tails with the experimental ones, are connected with the features of the vibrational excitation of the molecules as well as with the different probabilities of the dissociative neutralization on the different surfaces.

Molecular dynamics calculations demonstrate the existence of fragments overlapping energetically with the spectrum of scattered intact molecules. Under the conditions of axial surface channeling, considerable numbers of molecules are excited into the specific rotational propeller mode. These particles form a broad peak in the energy spectra, which essentially changes the shape of the total energy spectra at initial energies greater than 1500 eV.

Acknowledgment. This work was supported by the National Science Foundation through the Chemistry Division. The computational support was provided by the Center for Academic Computing at Penn State University. The experimental work is supported by the Deutsche Forschungsgemeinschaft (DFG).

References and Notes

(1) Heiland, W. in *Low Energy Ion Surface Interactions*; Rabalais, J. W., Ed.; Wiley: New York, 1994.
(2) Amirav, A. *Comments At. Mol. Phys*. **1990**, *24*, 187.
(3) Kleyn, A. W. *Vacuum* **1990**, *41*, 248.
(4) Närmann, A.; Franke, H.; Schmidt, K.; Arnau, A.; Heiland, W. *Nucl. Instrum. Methods B* **1992**, *69*, 158.
(5) Rechtien, J. H.; Harder, G.; Herrmann, G.; Röthig, C.; Snowdon, K. J. *Surf. Sci*. **1992**, *269/270*, 213.
(6) Bitensky, I. S.; Parilis, E. S. *Nucl. Instrum. Methods B* **1984**, *2*, 384.
(7) van Slooten, U.; Andersson, D.; Kleyn, A. W.; Gislason, E. A. *Chem. Phys. Lett*. **1991**, *185*, 440.
(8) Vicanek, M.; Schlathölter, T.; Heiland, W. *Nucl. Instrum. Methods B* **1997**, *125*, 194.
(9) Heiland, W.; Beitat, U.; Taglauer, E. *Phys. Rev. B.* **1977**, *19*, 1677.
(10) Snowdon, K. J. *Comments At. Mol. Phys*. **1994**, *30*, 93.
(11) Lorente, N.; Teillet-Billy, D.; Gauyacq, J.-P. *Nucl. Instrum. Methods B* **1999**, *157*, 1.
(12) Gadzuk, W.; Holloway, S. *Phys. Scripta* **1985**, *32*, 413.
(13) Willerding, B.; Heiland W.; Snowdon, K. J. *Phys. Rev. Lett*. **1984**, *53*, 2031.
(14) Tappe, W.; Niehof, A.; Schmidt, K.; Heiland, W. *Europhys. Lett*. **1991**, *15*, 405.
(15) Schins, J. M.; Vrijen, R. B.; van der Zande, W. J.; Los, J. *Surf. Sci*. **1993**, *280*, 145.
(16) Schmidt, K.; Schlathölter, T.; Närmann, A.; Heiland, W. *Chem. Phys. Lett.* **1992**, *200*, 465.
(17) Bitensky, I. S.; Ferleger, V. K.; Wojciechowski, I. A. *Nucl. Instrum. Methods B* **1997**, *125*, 214.
(18) Rechtien, J.-H.; Harder R.; Herrmann G.; Snowdon, K. J. *Surf. Sci*. **1992**, *272*, 240.
(19) Schlathölter, T.; Vicanek, M.; Heiland, W. *Surf. Sci*. **1996**, *195*, 352−354.
(20) Schlathölter, T.; Dirska M.; Närmann, A. *Radiat. Eff. Defects Solids* **1997**, *142*, 163.
(21) Brüning, K.; Heiland, W.; Schlathölter, T.; Wojciechowski, I. A.; Medvedeva, M. V.; Ferleger, V. Kh. *J. Chem. Phys*. **2000**, *113*, 2456.
(22) Wojciechowski, I. A.; Medvedeva, M. V.; Ferleger, V. Kh.; Brüning, K.; Heiland, W. *Nucl. Instrum. Methods B* **1998**, *143*, 473.
(23) Bitensky, I. S.; Gilenko, Ya. S.; Parilis, E. S. *Sov. Phys. JETP* **1988**, *67*, 470.
(24) Bitensky, I. S.; Parilis, E. S.; Wojciechowski, I. A. *Nucl. Instrum. Methods B* **1992**, *67*, 359.
(25) Winter, H. *Radiat. Eff*. **1990**, *117*, 53.
(26) Vicanek, M.; Schlathölter, T.; Heiland, W. *Nucl. Instrum. Methods B* **1997**, *125*, 194.
(27) Schlathölter, T.; Schlathölter, T.; Vicanek, M.; Heiland, W.; *J. Chem. Phys*. **1997**, *106*, 4723.
(28) Tappe, W.; Niehof, A.; Schmidt, K.; Heiland, W. *Europhys. Lett*. **1991**, *1991*, 405.
(29) Schins, J. M.; Vrijen, R. B.; van der Zande, W. J.; Los, J. *Surf. Sci*. **1993**, *280*, 145.
(30) Imke, U.; Snowdon, K. J.; Heiland, W. *Phys. Rev. B* **1984**, *43*, 41.
(31) Lorente, N.; Teilet-Billy, D.; Gauyacq, J.-P. *Surf. Sci*. **1998**, *197*, 402−404.
(32) Lorente, N.; Teilet-Billy, D.; Gauyacq, J.-P. *Nucl. Instrum. Methods B* **1999**, *157*, 1.
(33) Landau, L. D.; Lifshits, E. M.; *Statistical physics*, 2nd rev. ed.; Pergamon Press: New York, 1969; Part 1.
(34) Hausmann, S.; Höfner, C.; Schlathölter, T.; Franke, H.; Närmann, A.; Heiland, W. *Nucl. Instrum. Methods B* **1996**, *115*, 31.
(35) Höfner, C.; Närmann, A.; Heiland, W. *Nucl. Instrum. Methods B.* **1994**, *93*, 113.
(36) Baklitzky, B. E.; Bitensky, I. S. *Nucl. Instrum. Methods B* **1993**, *83*, 462.
(37) Garrison, B. J.; Winograd, N.; Daeven, D. M.; Reimann, C. T.; Lo, D. Y.; Tombrello, T. A.; Harrison, D. E. Jr.; Shapiro, M. N. *Phys. Rev. B* **1988**, *37*, 7197.
(38) Harrison, D. E. Jr. *CRC Crit. Rev. Solid State Mater. Sci.* **1988**, *14*, 51.
(39) Kelchner, C. L.; Halstead, D. M.; Perkins, L. S.; Wallace, N. M.; DePristo, A. E., *Surf. Sci.* **1994**, *310*, 425−435.
(40) Garrison, B. J.; Kodali, P. B. S.; Srivastava, D. *Chem. Rev*. **1996**, *96*, 1327.
(41) Sharp, T. E. *At. Data* **1971**, *2*, 119.
(42) Firsov, O. B. *Sov. Phys. JETP* **1958**, *6*, 534.
(43) Brüning, K. Ph.D. Thesis, Osnabrück 2000, http://marvin.physik.uni-osanbrueck.de/sp/theses.html.